

# Model-Based Sparse Source Identification

Reza Khodayi-mehr, Wilkins Aquino, and Michael M. Zavlanos

**Abstract**—This paper presents a model-based approach for source identification using sparse recovery techniques. In particular, given an arbitrary domain that contains a set of unknown sources and a set of stationary sensors that can measure a quantity generated by the sources, we are interested in predicting the shape, location, and intensity of the sources based on a limited number of sensor measurements. We assume a PDE model describing the steady-state transport of the quantity inside the domain, which we discretize using the Finite Element method (FEM). Since the resulting source identification problem is under-determined for a limited number of sensor measurements and the sought source vector is typically sparse, we employ a novel Reweighted  $\ell_1$  regularization technique combined with Least Squares Debiasing to obtain a unique, sparse, reconstructed source vector. The simulations confirm the applicability of the presented approach for an Advection-Diffusion problem.

## I. INTRODUCTION

Identifying sources from a limited number of measurements has many important applications. For example, identifying the source of underwater contaminants [1], [2], or leakage of hazardous substances [3], [4], is significant from an environmental protection and human-safety perspective. Source identification techniques can also be used to enable more complex tasks such as landmine clearing [5], or search-and-rescue missions and crowd evacuation in the case of emergencies [6].

Model-based source identification, where a PDE describes the transport phenomenon in a domain of interest, has been investigated previously, especially in the context of Advection-Diffusion models. The available methods can be classified depending on whether the sources are assumed to be functions with compact support in finite geometries or points in infinite space. While the latter methods often lead to closed-form solutions, the former are typically more general and can be used to address a broader range of problems. Further classifications are also possible depending on the number of sources, i.e., single vs. multiple, or on the state of the transport phenomenon, i.e., transient vs. steady-state. For example, localization of a single point-source in a steady-state transport system is considered in [7]. The source is assumed to be a delta or step function and the domain is assumed semi-infinite. Based on these assumptions, a closed-form solution for the forward problem is presented. This solution is then used to perform the localization task. On the other hand, localization of a single point-source in transient transport systems is considered in [5], [8]. The authors of [8] rely on *a priori* knowledge of the possible locations of the source or knowledge of the source's

intensity to solve the localization problem. A different approach is followed in [5] that uses statistical signal processing combined with closed-form solutions of the PDE transport models for infinite and rectangular domains to perform the source identification task.

The literature discussed above focuses on the identification of point-sources using closed-form solutions of the PDE transport models. Alternatively, optimization-based approaches can also be used to solve the underlying inverse problems. The authors of [9] use  $\ell_1$ -norm regularization to localize multiple instantaneous point-sources in a transient heat transfer system. A similar approach is followed in [10] where a sparse recovery method is formulated to identify multiple point-sources under steady-state conditions.

Assumptions of point-sources in infinite domains or assumptions on the intensity and number of these sources typically impose restrictions on the generality and applicability of the resulting methods. Sources of arbitrary shape in finite geometries are considered in [11], where a thresholding method based on sensitivity analysis of the objective functional is proposed to estimate the most likely location of the sources. The authors in [12] use FEM along with total variation regularization to solve the identification problem. Both of these methods appear to have low accuracy for small number of measurements.

In this paper, we address the identification problem for multiple sources with compact support inside an arbitrary domain at steady-state. After discretization of the PDE using the FEM, we obtain a linear model connecting the source and the measurable quantity. Then, our goal is to estimate the discrete source vector using a limited number of measurements inside the domain. The measurements are static and are taken at a small number of grid points of the FE mesh where the sensors are located. Assuming that the area occupied by the sources is much smaller compared to the whole domain, as is often the case in practice, the desired unknown source vector will be sparse which motivates the use of sparse reconstruction to estimate it. In this paper, we propose a novel algorithm to recover the solution of the source identification problem. Our method combines Reweighted  $\ell_1$  regularization (see, e.g., [13]) with Debiasing (see, e.g., [14]), to enhance the quality of the recovery. The use of FEM allows to handle different PDE models, multiple continuous sources, and arbitrary domain shapes, significantly increasing the applicability of our method. We show the effectiveness of the proposed method with simulations for an Advection-Diffusion problem.

The rest of this paper is organized as follows: In Section II, we discuss the Advection-Diffusion PDE under consideration and its discretization using FEM, and we formulate the proposed source identification problem as a sparse optimization

Reza Khodayi-mehr and Michael M. Zavlanos are with the Department of Mechanical Engineering and Materials Science, Duke University, Durham, NC 27708, USA, {reza.khodayi.mehr, michael.zavlanos}@duke.edu. Wilkins Aquino is with the Department of Civil and Environmental Engineering, Duke University, Durham, NC 27708, USA, wilkins.aquino@duke.edu.

problem. Section III, is devoted to the description of the proposed identification algorithm, its ingredients, and stopping criterion. In Section IV, numerical simulations are presented, while Section V contains the concluding remarks.

## II. PROBLEM FORMULATION

Let  $\Omega \subset \mathbb{R}^l$  be the domain of interest ( $1 \leq l \leq 3$ ), and assume the presence of sources is modeled by a function,  $f : \Omega \rightarrow \mathbb{R}_+$ , with compact support in the domain.<sup>1</sup> Let  $c : \Omega \rightarrow \mathbb{R}$  be the measurable quantity, such as concentration, generated by the sources. Moreover, let the velocity at which this quantity is transported via advection be  $\mathbf{v} \in \mathbb{R}^l$ , and  $D \in \mathbb{R}_+$  be the diffusivity of the medium. Under the steady-state assumption and applying a Dirichlet condition to the boundaries of the domain  $\partial\Omega$ , the governing Advection-Diffusion PDE will be of the form

$$\begin{aligned} \nabla \cdot (D\nabla c) - \nabla \cdot (\mathbf{v}c) + f &= 0, \\ c &= 0 \text{ on } \partial\Omega. \end{aligned} \quad (1)$$

Discretizing the PDE model (1) using FEM with  $n$  grid points we get the approximate model

$$\mathbf{K}\hat{\mathbf{c}} = \mathbf{R}\hat{\mathbf{f}}, \quad (2)$$

where the coefficient matrix  $\mathbf{K}$  and the matrix  $\mathbf{R}$  are  $n \times n$  sparse matrices whose dimension depends on the refinement of the mesh; see, e.g., [15]. In (2),  $\hat{\mathbf{f}}$  and  $\hat{\mathbf{c}}$  are the  $n$  dimensional source and concentration vectors, respectively, that satisfy the linear model (2). Assuming that the mesh is fine enough and  $n$  is large, we can neglect the discretization error and approximate the continuous variables  $c$  and  $f$  with their discrete peers  $\hat{\mathbf{c}}$  and  $\hat{\mathbf{f}}$  [15].

Consider now a set of  $m$  ( $m \ll n$ ) stationary sensors in the domain that measure the concentration  $\hat{\mathbf{c}}$  at the grid points of the FE mesh. Let  $\mathbf{y} \in \mathbb{R}^m$  be the vector of the measurements and assume that these measurements are contaminated by noise so that

$$\mathbf{y} = \mathbf{Q}(\hat{\mathbf{c}} + \mathbf{e}), \quad (3)$$

where  $\mathbf{e} \in \mathbb{R}^m$  is the noise vector and  $\mathbf{Q}$  is a  $m \times n$ , diagonal, binary, indicator matrix with ones at entries corresponding to the measurement locations and zero elsewhere. Then,  $\mathbf{y}$  has  $m$  nonzero entries corresponding to the sensor locations. Moreover, assume that the noise is white, i.e.,  $\mathbf{e} \sim \mathcal{N}(\mathbf{0}, \sigma^2\mathbf{I})$ , where  $\mathbf{I}$  denotes the identity matrix. Then, the source identification problem we address in this paper can be stated as follows:

**Problem 1.** *Given a possibly noisy measurement vector  $\mathbf{y} \in \mathbb{R}^m$ , calculate a vector  $\mathbf{x} \in \mathbb{R}^n$  that approximates the true source vector  $\hat{\mathbf{f}}$  as close as possible.*

Assuming any prediction of the source vector  $\mathbf{x}$  in place of  $\hat{\mathbf{f}}$ , we can solve (2) for the corresponding concentrations

<sup>1</sup>For the problem considered here, we assume that sources are strictly positive functions. In general, sources can also be negative in the case of sinks. Sinks can appear, e.g., in the presence of chemical reactions that consume a contaminant. The treatment of the problem in that case is similar.

$\mathbf{K}^{-1}\mathbf{R}\mathbf{x}$  and then left-multiply by the indicator matrix  $\mathbf{Q}$  to obtain the concentrations at the sensor locations as  $\mathbf{Q}\mathbf{K}^{-1}\mathbf{R}\mathbf{x}$ . Then, to solve Problem 1 we need to determine the source vector  $\mathbf{x}$  for which the concentrations  $\mathbf{Q}\mathbf{K}^{-1}\mathbf{R}\mathbf{x}$  match a given measurement vector  $\mathbf{y}$ , i.e., we need to solve

$$\mathbf{Q}\mathbf{K}^{-1}\mathbf{R}\mathbf{x} = \mathbf{y} \quad (4)$$

for the sought source vector  $\mathbf{x}$ . Since the number of measurements  $m$  is much smaller than the number of unknowns  $n$  ( $m \ll n$ ), the system of equations (4) is severely under-determined and does not have a unique solution. Moreover, due to the presence of noise in the measurement vector  $\mathbf{y}$ , any solution  $\mathbf{x}$  that satisfies the linear model (4) exactly, does not have a real physical meaning. Therefore, equation (4) cannot be used directly to solve the source identification problem. Instead, we employ an optimization-based approach that seeks the source vector  $\mathbf{x}$  for which the concentrations  $\mathbf{Q}\mathbf{K}^{-1}\mathbf{R}\mathbf{x}$  best approximate a given noisy measurement vector  $\mathbf{y}$  in a least-squares sense. In particular, we formulate the following problem

$$\min_{\mathbf{x} \geq \mathbf{0}} \|\mathbf{A}\mathbf{x} - \mathbf{y}\|_2^2, \quad (5)$$

where  $\mathbf{A} = \mathbf{Q}\mathbf{K}^{-1}\mathbf{R}$ . Note that the true source vector  $\hat{\mathbf{f}}$  is nonnegative, thus we introduce the constraint  $\mathbf{x} \geq \mathbf{0}$  in (5).

Since we do not measure the concentration at every grid point of the FE mesh, the least-squares problem (5) does not have a unique minimizer. To obtain a formulation that accepts a unique global minimizer as a solution, we introduce a regularization term in the objective and, therefore, we rewrite problem (5) as

$$\min_{\mathbf{x} \geq \mathbf{0}} \frac{1}{2} \|\mathbf{A}\mathbf{x} - \mathbf{y}\|_2^2 + \lambda R(\mathbf{x}), \quad (6)$$

where  $R(\mathbf{x})$  is the regularization term that ensures a unique solution for the original problem (5), and  $\lambda$  is the regularization parameter which balances between the data-fit and the regularization; see, e.g., [16]. Smaller values of  $\lambda$  mean more emphasis on the data-fit. Obviously, different choices of the regularization function  $R(\mathbf{x})$  will result in different solutions and this choice along with an appropriate value for  $\lambda$  is essential for acceptable recovery. The most popular choices for the regularization function are the norms  $\|\cdot\|_0$ ,  $\|\cdot\|_1$ ,  $\|\cdot\|_2$ , and the Total Variation  $TV(\cdot)$ . This regularization approach penalizes discontinuities and is observed to preserve sharp edges [17, section 8.6].

Since the area covered with sources is typically much smaller compared to the whole domain  $\Omega$ , we expect the discretized source vector  $\hat{\mathbf{f}}$  to be sparse. This motivates the use of the  $\ell_0$ -norm regularization to obtain a sparse solution to Problem 1. To avoid the non-convex and, therefore, computationally intractable nature of the resulting  $\ell_0$  regularized problem, we instead use a reweighted  $\ell_1$ -norm approach that has been recently proposed for the solution of sparse reconstruction problems [13]. The idea is to solve several weighted  $\ell_1$ -regularized problems iteratively and appropriately update

---

**Algorithm 1** Sparse Source Identification

---

**Require:** Measurements  $\mathbf{y}$ , matrix  $\mathbf{A}$ , and variance  $\sigma^2$ ;

**Require:** Regularization parameter  $\lambda$ ;

- 1: Initialize the iteration index  $k = 1$  and let  $\mathbf{x}_1 = \mathbf{0}$  and  $\mathbf{w}_1 = \mathbf{cons}$ ;
- 2: **while** the algorithm has not converged **do**
- 3: Solve for  $\hat{\mathbf{x}}_k$  the weighted  $\ell_1$ -regularized problem

$$\begin{aligned} \min_{\hat{\mathbf{x}}_k} \quad & 0.5 \|\mathbf{A}\hat{\mathbf{x}}_k - \mathbf{y}\|_2^2 + \lambda \mathbf{w}_k^T \hat{\mathbf{x}}_k \\ \text{s.t.} \quad & \hat{\mathbf{x}}_k \geq \mathbf{0}, \end{aligned}$$

for fixed weights  $\mathbf{w}_k$  and using  $\mathbf{x}_k$  as the initial value;

- 4: Solve for  $\bar{\mathbf{x}}_k$  the debiasing problem

$$\min_{\bar{\mathbf{x}}_k} 0.5 \|\mathbf{A}\bar{\mathbf{x}}_k - \mathbf{y}\|_2^2$$

s.t.  $[\bar{\mathbf{x}}_k]_i = 0$  if  $[\hat{\mathbf{x}}_k]_i = 0$  and  $[\bar{\mathbf{x}}_k]_i \geq 0$  if  $[\hat{\mathbf{x}}_k]_i \neq 0$ ,

using  $\hat{\mathbf{x}}_k$  as the initial value;

- 5: Set  $\mathbf{x}_{k+1} = \bar{\mathbf{x}}_k$ ;
  - 6: Update the weights  $\mathbf{w}_{k+1}$  using equation (8);
  - 7: Check the convergence criterion for  $\mathbf{x}_{k+1}$ ;
  - 8:  $k \leftarrow k + 1$ ;
  - 9: **end while**
- 

the weights of the regularization terms after every iteration. In particular, using the weighted  $\ell_1$ -norm as a regularization function, problem (6) becomes

$$\min_{\mathbf{x} \geq \mathbf{0}} \frac{1}{2} \|\mathbf{A}\mathbf{x} - \mathbf{y}\|_2^2 + \lambda \mathbf{w}^T \mathbf{x}, \quad (7)$$

where  $\mathbf{w}$  is a vector of weights. After every solution of problem (7) the vector  $\mathbf{w}$  is updated as

$$\mathbf{w}_i = \frac{1}{\mathbf{x}_i + \epsilon} \quad (8)$$

for all entries  $i = 1, \dots, n$ , where  $0 < \epsilon \ll \min\{x_i | x_i \neq 0\}$ .

Our proposed solution to Problem 1 combines sparse reconstruction (7) with data fit (5) in an iterative procedure, which we describe next.

### III. SPARSE SOURCE IDENTIFICATION ALGORITHM

Before discussing the details of the proposed algorithm, we reformulate problem (7) to the following Bound Constrained Quadratic Program:

$$\min_{\mathbf{x} \geq \mathbf{0}} \{J(\mathbf{x}) = \frac{1}{2} \mathbf{x}^T \mathbf{A} \mathbf{x} - \mathbf{c}^T \mathbf{x}\}, \quad (9)$$

where

$$\mathbf{A} = \mathbf{A}^T \mathbf{A}, \quad \mathbf{b} = \mathbf{A}^T \mathbf{y}, \quad \text{and} \quad \mathbf{c} = \mathbf{b} - \lambda \mathbf{w}. \quad (10)$$

For a fixed vector of weights  $\mathbf{w}$ , problem (9) is convex and efficient numerical methods exist to solve it. The algorithm we propose in this work is an iterative procedure, every iteration of which consist of three main phases. Phase I solves problem (9) for a fixed vector of weights  $\mathbf{w}$ . Phase II, called debiasing, solves the least-squares problem (5), trusting the

---

**Algorithm 2** Weighted  $\ell_1$  Regularization Phase

---

**Require:** Parameters  $\beta \in (0, 1)$ ,  $\mu \in (0, 0.5)$ ,  $\alpha_{min}$ ,  $\alpha_{max}$ ;

**Require:** Vector of weights  $\mathbf{w}_k$ ;

- 1: Initialize the iteration index  $s = 1$  and let  $\hat{\mathbf{x}}_k^1 = \mathbf{x}_k$ ;
- 2: **while** the algorithm has not converged **do**
- 3: Compute the step size  $\alpha$  using (12);
- 4: Set  $\alpha = \text{mid}(\alpha_{min}, \alpha, \alpha_{max})$ ;
- 5: Compute

$$\hat{\mathbf{x}}_k^{s+1} = (\hat{\mathbf{x}}_k^s - \alpha_s \nabla J(\hat{\mathbf{x}}_k^s))_+,$$

where  $\alpha_s$  is the first element of the sequence  $\{\alpha, \alpha\beta, \alpha\beta^2, \dots\}$  satisfying

$$J(\hat{\mathbf{x}}_k^{s+1}) \leq J(\hat{\mathbf{x}}_k^s) - \mu \nabla J(\hat{\mathbf{x}}_k^s)^T (\hat{\mathbf{x}}_k^s - \hat{\mathbf{x}}_k^{s+1});$$

- 6: Check the convergence criterion defined in (13);
  - 7:  $s \leftarrow s + 1$ ;
  - 8: **end while**
  - 9: Set  $\hat{\mathbf{x}}_k = \hat{\mathbf{x}}_k^s$ ;
- 

sparsity pattern obtained from the first phase. Finally, phase III updates the vector of weights  $\mathbf{w}$  according to equation (8). As discussed before, reweighting based on the current information about the solution enhances sparsity [13]. On the other hand, debiasing emphasizes the data-fit term and, therefore, improves on the reconstruction [14]. In Section IV we show that the proposed integrated method significantly enhances accuracy of the reconstruction.

Our method, containing the three phases, is shown in Algorithm 1. In this algorithm, the subscript  $k$  denotes the iteration index and the notation  $[\cdot]_i$  denotes the  $i$ -th component of a vector. The vector  $\mathbf{x}_k$  is the estimation of the true source vector  $\hat{\mathbf{f}}$  at iteration  $k$ , which also serves as an initial value for phase I in the next iteration of Algorithm 1. Line 3 in Algorithm 1 corresponds to phase I, which solves problem (9) for variable  $\hat{\mathbf{x}}_k$ , given a fixed vector of weights  $\mathbf{w}_k$  and using  $\mathbf{x}_k$  as an initial value. Line 4, corresponds to phase II, which solves the least-squares problem (5) for variables  $\bar{\mathbf{x}}_k$  using the solution  $\hat{\mathbf{x}}_k$  of phase I as an initial value. Finally, line 6 corresponds to phase III, which updates the vector of weights  $\mathbf{w}_{k+1}$  for the next iteration  $k + 1$  based on the solution  $\bar{\mathbf{x}}_k$  of the least-squares problem (5) at the current iteration  $k$ . In the following subsections, each of the three phases and the stopping criterion for Algorithm 1 are discussed.

#### A. Weighted $\ell_1$ Regularization

The first phase of Algorithm 1 is equivalent to problem (9) for fixed weights. To solve this problem, we use a gradient descent backtracking line-search method along with a gradient projection method; see, e.g., [14]. The proposed algorithm is an iterative procedure shown in Algorithm 2. We denote by  $s$  the iteration index of this algorithm and by  $\hat{\mathbf{x}}_k^s$  the resulting iterates corresponding to iteration  $k$  of Algorithm 1. In Algorithm 2, the function  $\text{mid}(a, b, c) = a$  if  $b < a < c$ , and is used to prevent very small or large steps, which may

lead to divergence. Moreover, the operator  $(\cdot)_+$  denotes the projection of the solution to the nonnegative orthant and is used to maintain feasibility.

The gradient projection method, used in Algorithm 2, is a fast active set method for quadratic problems with bound constraints; see, e.g., [18, section 16.7]. The main idea of this method is to project the gradient to the feasible set and then minimize the objective function in two successive steps. For the case of nonnegativity constraints, this method consists of the following two steps corresponding to lines 3, 4, and 5 of Algorithm 2:

- (i) Project the gradient so that for a small Cauchy step, the solution stays in the feasible box (nonnegative orthant), i.e.,

$$[\mathbf{g}_s]_i = \begin{cases} [\nabla J(\hat{\mathbf{x}}_k^s)]_i, & \text{if } [\hat{\mathbf{x}}_k^s]_i > 0 \text{ or } [\nabla J(\hat{\mathbf{x}}_k^s)]_i < 0, \\ 0, & \text{otherwise,} \end{cases} \quad (11)$$

for all  $i = 1, \dots, n$ , where  $[\cdot]_i$  denotes the  $i$ -th entry of a vector. Then minimize the univariate function  $J(\hat{\mathbf{x}}_k^s - \alpha \mathbf{g}_s)$  along the descent direction  $-\mathbf{g}_s$ , which leads to the closed-form solution

$$\alpha = \frac{\mathbf{g}_s^T \mathbf{g}_s}{\mathbf{g}_s^T \mathbf{\Lambda} \mathbf{g}_s}. \quad (12)$$

This step serves as a good starting point for each iteration of algorithm 2 and prevents large infeasibilities.

- (ii) Solve problem (9) using a backtracking line-search method, with  $-\nabla J(\hat{\mathbf{x}}_k^s)$  as the search direction, while projecting the iterations of this line-search onto the nonnegative orthant to maintain feasibility.

The function  $J(\cdot)$  above denotes the objective function defined in (9) and  $\mathbf{\Lambda}$  is the Hessian of the objective function defined in (10).

Since problem (9) falls in the class of Linear Complementary Problems [19], we can use the following stopping criterion for Algorithm 2

$$\|\min\{\hat{\mathbf{x}}_k^s, \nabla J(\hat{\mathbf{x}}_k^s)\}\|_2 < tol_1, \quad (13)$$

for some user specified tolerance  $tol_1$ . Note that the minimum in this equation is taken element-wise.

### B. Debiasing

During the debiasing phase, our algorithm trusts the sparsity pattern obtained from phase I, discussed in section III.A, and finds the best possible fit of the measurement vector  $\mathbf{y}$  that respects this sparsity pattern. Therefore, during the debiasing phase, we solve the least-squares problem (5) subject to the constraints that fix the zero elements of the solution. To reach this goal, we use a modified version of the Conjugate Gradient method, as described in Algorithm 3. We denote by  $s$  the iteration index of this algorithm and by  $\bar{\mathbf{x}}_k^s$  the resulting iterates corresponding to iteration  $k$  of Algorithm 1.

In this algorithm, the residual vector at iteration  $s$  is defined as  $\mathbf{r}_s = \mathbf{\Lambda} \bar{\mathbf{x}}_k^s - \mathbf{b}$ , where the Hessian matrix  $\mathbf{\Lambda}$  and the vector  $\mathbf{b}$  are the same as defined by (10) for problem (9). For a detailed derivation of the CG method see, e.g., [18, section 5.1]. In the

---

### Algorithm 3 Debiasing Phase

---

- 1: Initialize the iteration index  $s = 1$  and let  $\bar{\mathbf{x}}_k^1 = \hat{\mathbf{x}}_k$  and  $\mathbf{r}_1 = \mathbf{\Lambda} \bar{\mathbf{x}}_k^1 - \mathbf{b}$ ;
- 2: Calculate  $\bar{\mathbf{r}}_1$  from (14) and set  $\mathbf{p}_1 = -\bar{\mathbf{r}}_1$ ;
- 3: **while** the algorithm has not converged **do**
- 4:   Check the convergence criterion  $\|\bar{\mathbf{r}}_s\|_2^2 < tol_2$ ;
- 5:   Calculate

$$\alpha_s = \frac{\bar{\mathbf{r}}_s^T \bar{\mathbf{r}}_s}{\mathbf{p}_s^T \mathbf{\Lambda} \mathbf{p}_s},$$

$$\bar{\mathbf{x}}_k^{s+1} = (\bar{\mathbf{x}}_k^s + \alpha_s \mathbf{p}_s)_+,$$

$$\mathbf{r}_{s+1} = \mathbf{r}_s + \alpha_s \mathbf{p}_s;$$

- 6:   Calculate  $\bar{\mathbf{r}}_{s+1}$  from (14) and let

$$\beta_{s+1} = \frac{\bar{\mathbf{r}}_{s+1}^T \bar{\mathbf{r}}_{s+1}}{\bar{\mathbf{r}}_s^T \bar{\mathbf{r}}_s},$$

$$\mathbf{p}_{s+1} = -\bar{\mathbf{r}}_{s+1} + \beta_{s+1} \mathbf{p}_s;$$

- 7:    $s \leftarrow s + 1$ ;
  - 8: **end while**
  - 9: **Set**  $\bar{\mathbf{x}}_k = \bar{\mathbf{x}}_k^s$ ;
- 

modified CG method proposed in Algorithm 3, the values of the modified residual  $\bar{\mathbf{r}}_s$  are updated by

$$[\bar{\mathbf{r}}_s]_i = \begin{cases} [\mathbf{r}_s]_i, & \text{if } [\bar{\mathbf{x}}_k^1]_i \neq 0, \\ 0, & \text{otherwise,} \end{cases} \quad (14)$$

for all  $i = 1, \dots, n$ , where  $[\cdot]_i$  denotes the  $i$ -th entry of a vector. Equation (14) manipulates the residual vector  $\mathbf{r}_s$  to prevent the zero entries of the initial solution  $\bar{\mathbf{x}}_k^1$  to change. In order to speed up the debiasing Algorithm 3, we use gradient projection as in (11) to compute the residual  $\mathbf{r}_s$ .

Since the measurements  $\mathbf{y}$  are noisy, obtaining a perfect least-squares fit does not have a real physical meaning. Moreover, the conjugate gradient method itself serves as an iterative regularization process and needs proper termination, as discussed in [17, section 6.3]. Therefore, Algorithm 3 needs to terminate when the fit reaches a tolerance level  $tol_2$  which depends on the variance  $\sigma^2$  of the noise components. To estimate the appropriate value for  $tol_2$ , we first provide an expression for the expected value of  $\|\bar{\mathbf{r}}\|_2^2$ .

**Proposition 1.** *If the solution vector equals the true source vector, i.e.,  $\mathbf{x} = \hat{\mathbf{f}}$ , and the noise vector defined in (3) is white with distribution  $\mathbf{e} \sim \mathcal{N}(\mathbf{0}, \sigma^2 \mathbf{I})$ , then for the modified residual vector  $\bar{\mathbf{r}}$  defined by (14), we have*

$$\mathbb{E}\{\|\bar{\mathbf{r}}\|_2^2\} = \sigma^2 \text{tr}(\mathbf{Q} \mathbf{A}^T \mathbf{A}). \quad (15)$$

*Proof:* The proof follows from the formula for the expectation of the quadratic form. ■

If the problem is dominated by diffusion, i.e., if  $\mathbf{v} = \mathbf{0}$ , with constant diffusivity  $D$  and if the FE mesh is structured, then the nonzero entries of  $\mathbf{A}$  are identical except for the ones that correspond to the grid points at the boundaries of the domain  $\Omega$ . Consequently, we can use the approximation  $\text{tr}(\mathbf{Q} \mathbf{A}^2) \approx$

$m[\mathbf{A}]_j^T[\mathbf{A}]_j$ , where,  $m$  is the number of sensor measurements and  $[\mathbf{A}]_j$  is the  $j$ -th column of  $\mathbf{A}$ , where  $j = \lfloor \frac{n}{2} \rfloor$  is the index of the middle column of  $\mathbf{A}$  and  $\lfloor \cdot \rfloor$  is the floor function. On the other hand, for more general cases this approximation is not valid. We compensate for this approximation by using a safety factor  $\kappa \geq 1$  and, therefore, propose the following general rule to specify a value for  $tol_2$ :

$$tol_2 = \kappa m \sigma^2 [\mathbf{A}]_j^T [\mathbf{A}]_j. \quad (16)$$

### C. Regularization Parameter and Stopping Criterion

In this section, we discuss the selection of the initial constant vector of weights  $\mathbf{w}_1$ , and the regularization parameter  $\lambda$  for Algorithm 1. Moreover, we discuss a stopping criterion for this algorithm.

During the first iteration, when there is no information available about the sparsity in hand, Algorithm 1 starts by using constant regularization weights which are equal for all components. The value  $\lambda \mathbf{w}_1 = (0.05 \|\mathbf{A}^T \mathbf{y}\|_\infty) \mathbf{1}$ , is known to serve as a good starting value for the regularization weights [16], where  $\|\mathbf{x}\|_\infty = \max_i |x_i|$  and  $\mathbf{1} = [1 \dots 1]^T$ .

During the following iterations, an appropriate value for the regularization parameter  $\lambda$  is necessary. Since Algorithm 1 is initialized with the zero vector, i.e.,  $\mathbf{x}_1 = \mathbf{0}$ , the value of the regularization term in (7) varies from zero at the first iteration to ideally  $\|\hat{\mathbf{f}}\|_0$  upon convergence. On the other hand, the value of the data-fit term varies from  $\|\mathbf{y}\|_2^2$  in the first iteration to ideally  $\|\mathbf{e}\|_2^2$ . As a result, the value of the data-fit term changes for different measurement vectors  $\mathbf{y}$ , while the value of regularization term only depends on the sparsity of the source vector and is independent of  $\mathbf{y}$ . In order to incorporate the effect of  $\mathbf{y}$  in the regularization term, we use the heuristic value

$$\lambda = \alpha \|\mathbf{y}\|_2, \quad (17)$$

which works well in practice for a sufficiently large range of problem parameters, e.g., size and geometry.

Since the sparsity pattern of the solution is preserved when the iterates have converged to the optimal point, we can use sparsity as a sufficient stopping criterion of Algorithm 1 at line 7. The number of iterations screened for stopping depends on the relative number of unknowns and measurements  $n/m$ , and the noise level measured by the variance  $\sigma^2$  of the noise components.

## IV. NUMERICAL SIMULATIONS

In this section, we provide two numerical simulations, using MATLAB, to support the performance of the proposed algorithm and draw some conclusions based on the results. We refer to the method introduced in this paper as *RWDL*<sub>1</sub>. For the purpose of simulations, the domain is assumed to be a square area with unit length and an array of  $m$  sensors, distributed equidistantly in the domain, is used to gather the measurements  $\mathbf{y}$ .

In the following simulations, the error in the estimated source vector  $\mathbf{x}$ , compared to the true value  $\hat{\mathbf{f}}$ , is calculated as  $err = \|\mathbf{x} - \hat{\mathbf{f}}\|_2 / \|\hat{\mathbf{f}}\|_2$ , and the signal to noise ratio (*SNR*) is

defined as  $SNR = 10 \log(\sigma_{signal}^2 / \sigma_{noise}^2)$ , where  $\sigma_{signal}^2$  and  $\sigma_{noise}^2$  are the variances of the measurement vector  $\mathbf{y}$  and the noise vector  $\mathbf{e}$ , respectively. Moreover, sparsity is defined as  $sp = k/n$  and sampling-ratio is defined as  $sr = m/k$ , where  $k = \|\hat{\mathbf{f}}\|_0$  and  $m$  is the number of sensor measurements.

### A. Comparison with other Methods

In this section, we compare four regularization methods,  $\ell_2$ ,  $\ell_1$ , *TV*, and *RWDL*<sub>1</sub>, for a diffusion-dominated problem ( $D = 1$  and  $\mathbf{v} = \mathbf{0}$ ) with  $n = 41 \times 41 = 1681$  unknowns. For the  $\ell_1$  and *TV* regularization methods, popular implementations from [16] and [20] are used and tuning is done to get the best performance. The support of the source function, defined in equation (1), forms two rectangular, constant regions. The discretized source vector  $\hat{\mathbf{f}}$  has  $k = 61$  nonzero entries. Therefore, the source vector is very sparse and  $sp = 3.63\%$ .

In Table I, the results for different numbers of sensors and measurement noise levels are shown. The results show that *RWDL*<sub>1</sub> outperforms the other methods in terms of accuracy. Except for the  $\ell_2$ -regularization for which there exists a closed-form solution, the other methods are iterative. Among these methods, *RWDL*<sub>1</sub> takes the shortest time to solve the problem. It is notable that for the case of a  $7 \times 7$  sensor array, the problem is solved with under-sampling ( $sr < 1$ ).

For each case, an approximation of the tolerance  $tol_2$  is obtained using equation (16) with  $\kappa = 1$ . However, in order to improve on the performance, further tuning is required. Note that in the extreme case of noise-free data, the ideal value of  $tol_2$  is zero. Therefore, using smaller values of  $tol_2$  for this case can result in more accurate solutions at the cost of longer simulation times. For instance, setting  $tol_2 = 10^{-30}$  for the case of  $7 \times 7$  sensor array, the error value reduces from 17.86% to 2.16%, while the required simulation time increases from 1.38s to 3.41s. For large-scale problems the increase in time becomes more significant. Another important observation obtained from Table I is that the value of  $\alpha$  defined in equation (17) is almost constant, i.e.,  $\alpha \approx 0.2$ , for the source strength used in the current experiment for which  $max(\hat{\mathbf{f}}) = 10^4$ .

### B. Advection-Diffusion Transport

For this experiment, a FE mesh with  $n = 51 \times 51 = 2601$  unknowns is considered. A constant, rectangular source with intensity  $1.5 \times 10^4$  is used which results in a discrete source vector  $\hat{\mathbf{f}}$  with 66 nonzero entries ( $sp = 2.54\%$ ). Moreover, an array of  $7 \times 7$  sensors is assumed to take the measurements ( $sr < 1$ ). The transport phenomenon happens via advection with  $\mathbf{v} = [-10 \ 10]^T$ , and diffusion with  $D = 1$ .

For the noise-free case, with  $\alpha = 0.35$  and  $tol_2 = 10^{-30}$ , the estimation error is 11.44%. On the other hand, for the noisy case, with  $\sigma = 0.1$  and  $SNR = 47.79$ , the error is 26.56%. The values  $\alpha = 0.35$  and  $tol_2 = 10^{-8}$  are used (equation (16) gives  $tol_2 = 10^{-7}$ ). Figure 1 depicts the recovered source vector for the noisy measurements.

## V. CONCLUSION

In this paper, we considered the problem of model-based source identification using the sparse recovery techniques.

TABLE I  
COMPARISON WITH OTHER POPULAR REGULARIZATION METHODS

$m$	$\sigma$	$SNR$	$\ell_2$		$\ell_1$		$TV$		$RWDL_1$			
			$err(\%)$	$t(s)$	$err(\%)$	$t(s)$	$err(\%)$	$t(s)$	$\alpha$	$tol_2$	$err(\%)$	$t(s)$
$7 \times 7$	0	$\infty$	60.00	0.09	52.22	5.67	35.09	7.88	0.2	$10^{-16}$	17.86	1.38
	0.1	50.56	60.03	0.08	52.22	6.43	36.05	7.61	0.2	$10^{-8}$	27.85	2.05
	1	28.15	62.67	0.09	58.61	6.63	44.64	8.08	0.3	$10^{-4}$	34.11	1.03
$10 \times 10$	0	$\infty$	45.55	0.10	41.70	13.1	12.93	7.75	0.1	$10^{-16}$	0.64	2.55
	0.1	48.74	44.82	0.09	41.34	13.3	17.54	7.54	0.25	$10^{-7}$	9.90	1.84
	1	29.84	61.41	0.09	63.23	12.94	57.95	8.40	0.2	$10^{-3}$	37.50	1.90

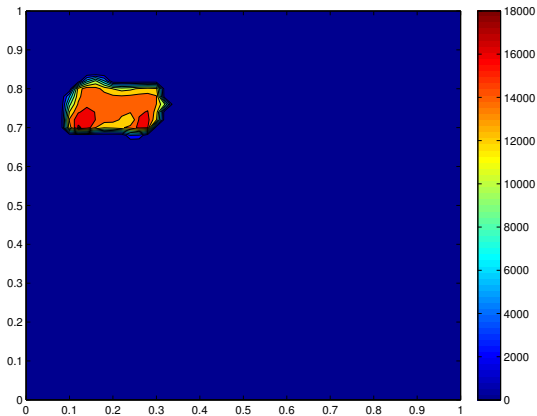


Fig. 1. Plot of the solution of advection-diffusion identification problem in the presence of noise with  $SNR = 47.79$ . The reconstruction error is 26.56%.

Given a domain with unknown sources inside it, we proposed an algorithm to determine the number and characteristics of these sources. We used a PDE-model to describe the transport of the measurable quantity generated by the sources. Then, we discretized the PDE-model using FEM which gives the flexibility to deal with different models, multiple sources with compact support, and arbitrary domains. Since for limited number of measurements the problem is under-determined and based on the fact that the discretized source vector is sparse, we used a reweighted  $\ell_1$ -regularization technique combined with a debiasing phase to solve the identification problem. We demonstrated the effectiveness of our proposed method in the numerical simulations. We showed that our method outperforms some popular regularization approaches that are often used in the literature.

## REFERENCES

- [1] F. B. Belgacem, "Identifiability for the pointwise source detection in fisher's reaction-diffusion equation," *Inverse Problems*, vol. 28, no. 6, p. 065015, 2012. [Online]. Available: <http://stacks.iop.org/0266-5611/28/i=6/a=065015>
- [2] A. E. Badia, T. Ha-Duong, and A. Hamdi, "Identification of a point source in a linear advection-dispersion-reaction equation: application to a pollution source problem," *Inverse Problems*, vol. 21, no. 3, p. 1121, 2005. [Online]. Available: <http://stacks.iop.org/0266-5611/21/i=3/a=020>
- [3] A. S. Kalelkar, *Investigation of large-magnitude incidents: Bhopal as a case study*. Arthur D. Little, Incorporated, 1988.
- [4] F. Berkhout, "Radioactive waste management: by Y.S. Tang and J.H. Saling, Taylor and Francis, Basingstoke, 1990, 460 pp," *Energy Policy*, vol. 20, no. 3, pp. 275 – 276, 1992. [Online]. Available: <http://www.sciencedirect.com/science/article/pii/030142159290088J>
- [5] A. Jeremic and A. Nehorai, "Landmine detection and localization using chemical sensor array processing," *Signal Processing, IEEE Transactions on*, vol. 48, no. 5, pp. 1295–1305, May 2000.
- [6] E. Lee, "Clinical manifestations of Sarin nerve gas exposure," *JAMA*, vol. 290, no. 5, pp. 659–662, 2003. [Online]. Available: [+http://dx.doi.org/10.1001/jama.290.5.659](http://dx.doi.org/10.1001/jama.290.5.659)
- [7] J. Matthes, L. Groll, and H. Keller, "Source localization by spatially distributed electronic noses for advection and diffusion," *Signal Processing, IEEE Transactions on*, vol. 53, no. 5, pp. 1711–1719, May 2005.
- [8] M. Alpay and M. Shor, "Model-based solution techniques for the source localization problem," *Control Systems Technology, IEEE Transactions on*, vol. 8, no. 6, pp. 895–904, Nov 2000.
- [9] Y. Li, S. Osher, and R. Tsai, "Heat source identification based on  $\ell_1$  constrained minimization," UCLA CAM Report, Tech. Rep., 2011.
- [10] Y. Cheng and T. Singh, "Source term estimation using convex optimization," in *Information Fusion, 2008 11th International Conference on*, June 2008, pp. 1–8.
- [11] A. Sabelli and W. Aquino, "A source sensitivity approach for source localization in steady-state linear systems," *Inverse Problems*, vol. 29, no. 9, p. 095005, 2013. [Online]. Available: <http://stacks.iop.org/0266-5611/29/i=9/a=095005>
- [12] V. Akçelik, G. Birocs, O. Ghattas, K. R. Long, and B. v. B. Waanders, "A variational finite element method for source inversion for convective-diffusive transport," *Finite Elem. Anal. Des.*, vol. 39, no. 8, pp. 683–705, May 2003. [Online]. Available: [http://dx.doi.org/10.1016/S0168-874X\(03\)00054-4](http://dx.doi.org/10.1016/S0168-874X(03)00054-4)
- [13] E. J. Candès, M. B. Wakin, and S. P. Boyd, "Enhancing sparsity by reweighted  $\ell_1$  minimization," *Journal of Fourier Analysis and Applications*, vol. 14, no. 6, pp. 877–905, 2008.
- [14] M. Figueiredo, R. Nowak, and S. Wright, "Gradient projection for sparse reconstruction: Application to compressed sensing and other inverse problems," *Selected Topics in Signal Processing, IEEE Journal of*, vol. 1, no. 4, pp. 586–597, Dec 2007.
- [15] D. L. Logan, *A First Course in the Finite Element Method*. Nelson, 2007.
- [16] S.-J. Kim, K. Koh, M. Lustig, S. Boyd, and D. Gorinevsky, "An interior-point method for large-scale  $\ell_1$ -regularized least squares," *Selected Topics in Signal Processing, IEEE Journal of*, vol. 1, no. 4, pp. 606–617, Dec 2007.
- [17] P. C. Hansen, *Discrete Inverse Problems*. SIAM, 2010.
- [18] J. Nocedal and S. J. Wright, *Numerical Optimization*. New York: Springer-Verlag, 2006.
- [19] Y. Xiao, Q. Wang, and Q. Hu, "Non-smooth equations based method for  $\ell_1$ -norm problems with applications to compressed sensing," *Nonlinear Analysis: Theory, Methods and Applications*, vol. 74, no. 11, pp. 3570–3577, 2011. [Online]. Available: <http://www.sciencedirect.com/science/article/pii/S0362546X11001210>
- [20] E. Candès and J. Romberg, " $\ell_1$ -magic: A collection of matlab routines for solving the convex optimization programs central," *Compressive Sampling*, 2006.